

Analytic Modeling of the Xenon Oscillation Due to Control Rod Movement

Jae Seung Song and Nam Zin Cho

Korea Advanced Institute of Science and Technology
373-1 Kusong-dong, Yusong-gu, Taejon, 305-701, Korea

Sung Quun Zee

Korea Atomic Energy Research Institute
150 Dukjin-dong, Yusong-gu, Taejon, 305-600, Korea

(Received July 6, 1998)

Abstract

An analytic axial xenon oscillation model was developed for pressurized water reactor analysis. The model employs an equation system for axial difference parameters that was derived from the two-group one-dimensional diffusion equation with control rod modeling and coupled with xenon and iodine balance equations. The spatial distributions of flux, xenon, and iodine were expanded by the Fourier sine series, resulting in cancellation of the flux-xenon coupled non-linearity. An inhomogeneous differential equation system for the axial difference parameters, which gives the relationship between power, iodine and xenon axial differences in the case of control rod movement, was derived and solved analytically. The analytic solution of the axial difference parameters can directly provide with the variation of axial power difference during xenon oscillation. The accuracy of the model is verified by benchmark calculations with one-dimensional reference core calculations.

1. Introduction

Xenon-induced spatial power oscillations occur as a result of rapid perturbations to the power distribution that cause the xenon and iodine distributions to be out of phase with the perturbed power distribution. This results in a shift in the xenon and iodine distributions that causes the power distribution to change in an opposite

direction from the initial perturbation, and thus an oscillatory condition is established. The xenon-induced power oscillation is described by a system of differential equations with non-linearities between xenon and flux distributions. Many approaches[1-7] to analyze the equations had been proposed using linear modal analysis which generally proceeds by linearizing the equations and expanding the spatial dependence in terms of

eigenfunctions. However, these focused on derivations of stability criteria because the stability is relatively easy to evaluate by derivations of transfer functions, while the explicit spatial solutions are too complex and difficult to obtain analytically. Onega and Kisner[8,9] developed a two-point xenon oscillation model. The model employed the non-linear xenon and iodine balance equations coupled with one-group neutron diffusion equation having non-linear power reactivity feedback. The non-linearity was treated explicitly but only numerical results of spatial oscillation were given. Cho and Grossman[10] developed a simple core control model for the control of xenon spatial oscillation. The model was formulated as a linear-quadratic tracking problem and the resulting two-point boundary problem was solved directly.

Recently, an analytical model was proposed, which provides complete analytic solutions for the xenon oscillation characteristics.[11-12] The axial xenon oscillation is characterized by axial difference parameters which are based on Fourier sine series expansions of the spatial distributions of flux, xenon, and iodine. Through this approach, the xenon-flux coupled non-linear terms were completely linearized and an analytical solution for the axial power difference was derived. In this model, the xenon oscillation behavior is described by a homogeneous equation system of axial difference parameters which does not include the control rod movement in the core.

This study is an extension of the above analytic xenon oscillation model to treat the control rod movements in the core. With the control rod movements, the equation system of the xenon oscillation becomes inhomogeneous. The solution of the xenon oscillation characteristics with control rod modeling is provided. The model was benchmarked by reference calculations based on the two-group one-dimensional neutron diffusion

theory code ONED94.[13]

2. Equation of Axial Difference Parameters

2.1. Derivation of a System of Equations for Axial Difference Parameters

The equation treatment of this study is similar to those of previous work[12] except that the control rod considerations are included. However, for completeness of our discussion all of the processes are reproduced herein. The two-group one-dimensional diffusion equations with xenon dynamics including control rod modeling are given by

$$0 = \frac{d}{dz} D_1(z) \frac{d}{dz} \varphi_1(z, t) - \Sigma_1(z) \varphi_1(z, t) + \frac{1}{k} [\nu \Sigma_{f1}(z) \varphi_1(z, t) + \frac{\tilde{\phi}_2}{\tilde{\phi}_1} \nu \Sigma_{f2}(z) \varphi_2(z, t)] - \Delta \Sigma_{a1}(z, t) \varphi_1(z, t), \quad (1a)$$

$$0 = \frac{d}{dz} D_2(z) \frac{d}{dz} \varphi_2(z, t) - \Sigma_2^*(z) \varphi_2(z, t) + \frac{\tilde{\phi}_1}{\tilde{\phi}_2} \Sigma_R(z) \varphi_1(z, t) - \sigma_x \tilde{N}_x X(z, t) \varphi_2(z, t) + \alpha_p \varphi_2(z, t) - \Delta \Sigma_{a2}(z, t) \varphi_2(z, t), \quad (1b)$$

$$\frac{\partial I(z, t)}{\partial t} = -\lambda_I I(z, t) + \frac{\gamma_I}{\tilde{N}_I} [\Sigma_{f1}(z) \tilde{\phi}_1 \varphi_1(z, t) + \Sigma_{f2}(z) \tilde{\phi}_2 \varphi_2(z, t)], \quad (1c)$$

$$\frac{\partial X(z, t)}{\partial t} = -\lambda_x X(z, t) - \sigma_x \tilde{\phi}_2 \varphi_2(z, t) X(z, t) + \lambda_I \frac{\tilde{N}_I}{\tilde{N}_x} I(z, t) + \frac{\gamma_x}{\tilde{N}_x} [\Sigma_{f1}(z) \tilde{\phi}_1 \varphi_1(z, t) + \Sigma_{f2}(z) \tilde{\phi}_2 \varphi_2(z, t)], \quad (1d)$$

where

$\tilde{\phi}_g, \tilde{N}_x, \tilde{N}_I$ = Core average values of group-wise flux, xenon, and iodine number densities, respectively,

$\varphi_g(z, t)$ = group-wise neutron flux distribution,

$X(z, t)$ = xenon distribution,

$I(z, t)$ = iodine distribution,

α_p = power coefficient in units of change in neutron production rate per unit power change per unit thermal flux,
 $\Sigma_2^*(z) = \Sigma_{a2}(z, t) - \sigma_X X(z, t)$,
 $\Sigma_1(z) = \Sigma_{a1}(z) + \Sigma_R(z)$,
 $\Delta \Sigma_{ag}(z, t)$ = control rod absorption cross sections of energy group g ,

and other notations are standard. It is assumed that power and xenon feedbacks affect only the thermal neutron balance and the core properties do not change during the xenon oscillation except the thermal neutron absorption due to the change of xenon distribution. The power feedback is represented as the power coefficient multiplied by the thermal flux, as in the concept of Stacey's power feedback model.[6]

Now the one-dimensional spatial distribution for the i -th parameter is expanded by Fourier sine series as

$$y_i(z, t) = \sum_{n=1}^{\infty} b_{i,n}(t) \sin\left(\frac{n\pi z}{H}\right), \quad (2)$$

where H is the effective core height. By this expansion each axial difference parameter, which is defined by the difference in the parameter between the bottom and top half cores, has only the $(4k-2)$ nd terms as follows:

$$Z_i(t) = \int_0^{H/2} y_i(z, t) dz - \int_{H/2}^H y_i(z, t) dz = \sum_{k=1}^{\infty} \frac{2H}{(2k-1)\pi} b_{i,(4k-2)}(t). \quad (3)$$

Therefore, if we are interested in the axial difference parameters, the approximation of Fourier series expansion with only the first and second terms for the spatial distribution has the accuracy equivalent to the Fourier series expansion with five terms. The spatial distribution of Eq. (2) is normalized so that the core average value is equal to 1.0,

$$\frac{\int_0^H [b_1 \sin(\frac{\pi z}{H}) + b_2 \sin(\frac{2\pi z}{H})] dz}{\int_0^H dz} = 1. \quad (4)$$

If we solve this equation, the coefficient of the first Fourier sine term satisfies the condition of

$$b_1 = \frac{\pi}{2}. \quad (5)$$

By the above approximation, the eigenvalue k in Eq. (1a) should be reproduced by integration of the equation over the core height as

$$k = \frac{v\tilde{\Sigma}_{f1} + \frac{\tilde{\phi}_2}{\tilde{\phi}_1} v\tilde{\Sigma}_{f2}}{(\frac{\pi}{H})^2 \tilde{D}_1 + \tilde{\Sigma}_1}, \quad (6)$$

where the sign \sim means core average quantities. Let cross sections homogenized for each half core be

$$\Sigma_{i,B} = \frac{\int_0^{H/2} \Sigma_i(z) \phi(z) dz}{\int_0^{H/2} \phi(z) dz} \quad \text{and} \quad \Sigma_{i,T} = \frac{\int_{H/2}^H \Sigma_i(z) \phi(z) dz}{\int_{H/2}^H \phi(z) dz}. \quad (7)$$

It is assumed that the cross section change due to control rod motion is only step function at the top half core only, i.e.,

$$\Delta \Sigma_{i,B}(t) = 0 \quad \text{and} \quad \Delta \Sigma_{i,T}(t) = \Delta \Sigma_{ai}. \quad (8)$$

Now, an operator is defined to calculate the difference of integrals between the bottom and top half cores as follows.

$$\Theta(Y) = \left[\int_0^{H/2} Y dz - \int_{H/2}^H Y dz \right], \quad (9)$$

so that $b_{i,2}$ denotes the axial difference parameter itself, because the coefficients of Fourier series are already normalized by Eqs. (4) and (5). The differences of unknowns from those at the equilibrium condition is defined by

$$E_i = b_{i,2}(t) - b_{i,2}(\infty), \quad (10)$$

where index i represents fast flux, thermal flux,

iodine and xenon for 1, 2, 3 and 4, respectively.

Inserting Eq. (5) into Eqs. (1) through (4), then the operation Θ results in

$$\underline{\mathbf{D}} = \underline{\mathbf{C}} \underline{\mathbf{E}} + \underline{\mathbf{A}}, \quad (11)$$

where

$$\underline{\mathbf{D}}^T = (0, 0, \frac{dE_3(t)}{dt}, \frac{dE_4(t)}{dt}),$$

$$\underline{\mathbf{E}}^T = (E_1(t), E_2(t), E_3(t), E_4(t)),$$

$$\underline{\mathbf{A}}^T = \left(-\frac{\pi}{4} \Delta \Sigma_{a1}, -\frac{\pi}{4} \Delta \Sigma_{a2}, 0, 0 \right),$$

$$\underline{\mathbf{C}} = \begin{bmatrix} \left(\begin{array}{c} 4\pi^2 \bar{D}_1 \\ H^2 \\ \bar{v} \bar{\Sigma}_f \bar{f}_1 + \frac{\Delta \Sigma_{a1}}{2} \end{array} \right) & \frac{\bar{v} \bar{\Sigma}_f \bar{\phi}_2}{k \bar{\phi}_1} & 0 & 0 \\ \frac{\bar{\Sigma}_R \bar{\phi}_1}{\bar{\phi}_2} & \left(\begin{array}{c} 4\pi^2 \bar{D}_2 + \frac{\pi \sigma_X \bar{N}_X}{3} \\ H^2 \\ -\bar{\Sigma}_2 + \alpha_p + \frac{\Delta \Sigma_{a2}}{2} \end{array} \right) & 0 & -\frac{\pi \sigma_X \bar{N}_X}{3} \\ \frac{\gamma_1 \bar{\Sigma}_f \bar{\phi}_1}{\bar{N}_I} & \frac{\gamma_1 \bar{\Sigma}_f \bar{\phi}_2}{\bar{N}_I} & -\lambda_1 & 0 \\ \frac{\gamma_X \bar{\Sigma}_f \bar{\phi}_1}{\bar{N}_X} & \left(\frac{\gamma_X \bar{\Sigma}_f \bar{\phi}_2}{\bar{N}_X} - \frac{\pi \sigma_X \bar{\phi}_2}{3} \right) & \frac{\lambda_1 \bar{N}_I}{\bar{N}_X} & \left(-\lambda_X - \frac{\pi \sigma_X \bar{\phi}_2}{3} \right) \end{bmatrix}$$

$$\bar{D}_i = \frac{\bar{D}_{i,B} + \bar{D}_{i,T}}{2}, \quad \text{and} \quad \bar{\Sigma}_i = \frac{\bar{\Sigma}_{i,B} + \bar{\Sigma}_{i,T}}{2}.$$

It should be noted that cross sections appearing in the above equations are not core average values, which are usually defined by the flux weighted averages, but the arithmetic average of the homogenized cross sections for the bottom and top halves of the core. However, the two quantities are usually close to each other in operating reactors.

2.2. Solution of the System of Equations for Axial Difference Parameters

In order to obtain complete solutions, each initial condition of $E_i(t=0)$ is required. However, all of the parameters such as flux, iodine and xenon distributions are not measurable in power reactors. Therefore, the initial conditions should be estimated from the axial power difference which can directly be measured. Also note that the axial power difference may be the parameter in which we are usually interested. Let $E_p(t)$ be the difference of the axial power difference from that of the equilibrium condition in a relative power unit, then

$$E_p(t) = f_1 E_1(t) + f_2 E_2(t), \quad (12)$$

where

$$f_1 = \frac{\kappa \Sigma_{f1} \bar{\phi}_1}{\kappa \Sigma_{f1} \bar{\phi}_1 + \kappa \Sigma_{f2} \bar{\phi}_2} \quad \text{and} \quad f_2 = \frac{\kappa \Sigma_{f2} \bar{\phi}_2}{\kappa \Sigma_{f1} \bar{\phi}_1 + \kappa \Sigma_{f2} \bar{\phi}_2},$$

which implies the power fraction contributed by each group flux. Combining Eqs. (11) and (12) we can get an equation system which represent the relationship of axial difference parameters as follows:

$$0 = C_{p2} E_p + C_{24} E_4 + A'_2 \quad (13a)$$

$$\frac{dE_3}{dt} = C_{p3} E_p + C_{33} E_3 + A'_3 \quad (13b)$$

$$\frac{dE_4}{dt} = C_{p4} E_p + C_{43} E_3 + C_{44} E_4 + A'_4 \quad (13c)$$

where

$$C_{p2} = \frac{C_{12} C_{21} - C_{11} C_{22}}{f_1 C_{12} - f_2 C_{11}}, \quad A'_2 = \frac{C_{21} f_2 - C_{22} f_1}{f_1 C_{12} - f_2 C_{11}} A_1 + A_2,$$

$$C_{p3} = \frac{C_{12} C_{31} - C_{11} C_{32}}{f_1 C_{12} - f_2 C_{11}}, \quad A'_3 = \frac{C_{31} f_2 - C_{32} f_1}{f_1 C_{12} - f_2 C_{11}} A_1,$$

$$C_{p4} = \frac{C_{12}C_{41} - C_{11}C_{42}}{f_1C_{12} - f_2C_{11}}, \quad A'_1 = \frac{C_{41}f_2 - C_{42}f_1}{f_1C_{12} - f_2C_{11}} A_1,$$

In the equilibrium state, Eqs. (13) are

$$0 = C_{p2}E_p(\infty) + C_{24}E_4(\infty) + A'_2, \quad (14a)$$

$$0 = C_{p3}E_p(\infty) + C_{33}E_3(\infty) + A'_3, \quad (14b)$$

$$0 = C_{p4}E_p(\infty) + C_{43}E_3(\infty) + C_{44}E_4(\infty) + A'_4, \quad (14c)$$

which give the difference of the axial power difference between rodged and unrodged equilibrium states as follows :

$$E_p(\infty) = -\frac{A'_2C_{33}C_{44} + C_{24}(A'_3C_{43} - A'_4C_{33})}{C_{33}C_{44}C_{p2} + C_{24}(C_{43}C_{p3} - C_{33}C_{p4})}, \quad (15a)$$

$$E_3(\infty) = \frac{C_{44}(A'_2C_{p3} - A'_3C_{p2}) + C_{24}(A'_3C_{p4} - A'_4C_{p3})}{C_{33}C_{44}C_{p2} + C_{24}(C_{43}C_{p3} - C_{33}C_{p4})}, \quad (15b)$$

$$E_4(\infty) = \frac{C_{44}(A'_2C_{p3} - A'_3C_{p2}) + C_{24}(A'_3C_{p4} - A'_4C_{p3})}{C_{33}C_{44}C_{p2} + C_{24}(C_{43}C_{p3} - C_{33}C_{p4})} \quad (15c)$$

For easy treatment of Eqs. (13), the ASI difference from rodged equilibrium state is defined by

$$R_i(t) = E_i(t) - E_i(\infty). \quad (16)$$

Inserting Eq. (16) into Eqs. (13a) through (13c), we can get

$$0 = C_{p2}R_p + C_{24}R_4, \quad (17a)$$

$$\frac{dR_3}{dt} = C_{p3}R_p + C_{33}R_3, \quad (17b)$$

$$\frac{dR_4}{dt} = C_{p4}R_p + C_{43}R_3 + C_{44}R_4. \quad (17c)$$

By Laplace transform

$$0 = C_{p2}\mathfrak{R}_p(s) + C_{24}\mathfrak{R}_4(s), \quad (18a)$$

$$s\mathfrak{R}_3(s) - R_3(0) = C_{p3}\mathfrak{R}_p(s) + C_{33}\mathfrak{R}_3(s), \quad (18b)$$

$$s\mathfrak{R}_4(s) - R_4(0) = C_{p4}\mathfrak{R}_p(s) + C_{43}\mathfrak{R}_3(s) + C_{44}\mathfrak{R}_4(s), \quad (18c)$$

where $\mathfrak{R}(s)$ is the Laplace transform of $\mathfrak{R}(t)$, and the solution of $\mathfrak{R}_p(s)$ is given by

$$\mathfrak{R}_p(s) = \eta \frac{(s-B)}{(s-B)^2 + \omega^2} + \xi \frac{\omega}{(s-B)^2 + \omega^2}, \quad (19)$$

where

$$B = \frac{1}{2}(C_{33} + C_{44} - \frac{C_{24}C_{p4}}{C_{p2}}),$$

$$\omega^2 = -B^2 + C_{33}C_{44} + \frac{C_{24}}{C_{p2}}(C_{43}C_{p3} - C_{33}C_{p4}),$$

$$\eta = -\frac{C_{24}}{C_{p2}}R_4(0),$$

and

$$\xi = -\frac{C_{24}}{\omega C_{p2}}[C_{43}R_3(0) + (B - C_{33})R_4(0)].$$

Note that η and ξ can also be represented by initial conditions of power variation as

$$\eta = R_p(0) \quad (20a)$$

and

$$\xi = \frac{1}{\omega} \left[\frac{dR_p(t)}{dt} \Big|_{t=0} - BR_p(0) \right]. \quad (20b)$$

Equation (19) gives the solution of

$$R_p(t) = e^{Bt}[\eta \cos(\omega t) + \xi \sin(\omega t)] \quad (21)$$

and finally we can get

$$E_p(t) = E_\infty + e^{Bt}[\eta \cos(\omega t) + \xi \sin(\omega t)]. \quad (22)$$

The physical meaning of the final solution is that the initial power perturbation causes cosine shape oscillation due to xenon redistribution and the oscillation is affected by sine shape oscillation due to iodine redistribution. The iodine and xenon redistributions can be represented by the initial axial power difference perturbation and its derivative. The effect of control rod movement on the damping ratio and frequency of the oscillation is negligible.

One of the important facts is that the control rod effect on the oscillation can be represented by the rodged equilibrium axial power difference instead of the control rod cross sections. The rodged equilibrium ASI data can be predetermined much easier than the control rod cross sections. Thus, the initialization of iodine and xenon requires only unrodged equilibrium core parameters, iodine and xenon related physical constants, equilibrium rodged axial power difference, and initial power perturbation data.

3. Benchmarks

In order to test the accuracy of the analytical results, two reference xenon oscillations were generated via the two-group one-dimensional core calculation code ONED94.[13] The reference core model is the same core model in Table II of Reference 12. The physical constants of xenon and iodine, core average quantities and core average cross sections of the equilibrium xenon condition are reproduced in Table 1. In the first oscillation, a control bank insertion at an unrodged equilibrium core state, was simulated by ONED94. In the second oscillation, a control bank

Table 1. Data for Benchmark Problem

| Parameters | Unit | Values |
|------------------------------------|------------------------|--|
| H | cm | 381 |
| λ_I, λ_X | sec ⁻¹ | $2.924 \times 10^{-5}, 2.100 \times 10^{-5}$ |
| $\tilde{\beta}_1, \tilde{\beta}_2$ | #/cm ² -sec | $1.366 \times 10^{14}, 3.117 \times 10^{13}$ |
| \tilde{N}_I, \tilde{N}_X | #/cm ³ | $3.224 \times 10^{15}, 1.497 \times 10^{15}$ |
| D_1, D_2 | cm ⁻¹ | 1.320, 4.005×10^{-1} |
| Σ_{a1}, Σ_{a2} | cm ⁻¹ | $8.652 \times 10^{-3}, 7.480 \times 10^{-2}$ |
| Σ_R | cm ⁻¹ | 1.711×10^{-2} |
| Σ_{f1}, Σ_{f2} | cm ⁻¹ | $2.254 \times 10^{-3}, 3.772 \times 10^{-2}$ |
| ν | | 2.469 |
| σ_X | cm ² | 1.431×10^{-18} |
| α_P | cm ⁻¹ | -2.697×10^{-4} |
| ASI (ARO, Eq) | | 0.0278 |
| $E(\infty)$ (rodged) | | 0.0814 |

withdrawal at an control bank inserted equilibrium state was also simulated. Both control bank movement lead to an axial power perturbation followed by oscillation. Using the initial power perturbations and their derivatives of ONED94 results, the behaviors of oscillations are estimated by Eq. (22) and compared with the results of ONED94 simulations as shown in Figures 1 and 2. In this comparison the axial power is parameterized by axial shape index (ASI) defined by

$$ASI = \frac{P_B - P_T}{P_B + P_T}, \quad (23)$$

where P_B and P_T are the bottom and the top half powers of the core, respectively. The errors of oscillation period of the analytic estimation of Eq. (23) from the ONED94 reference results are only 0.25 hour for both benchmark cases. The errors of the second ASI peaks are 0.7 and 1.3 % ASI unit for the control rod insertion and withdrawal cases, respectively.

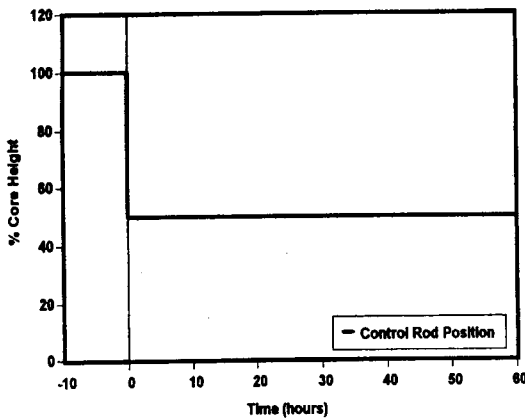


Fig. 1. Comparison of ASI Variation for Control Rod Insertion

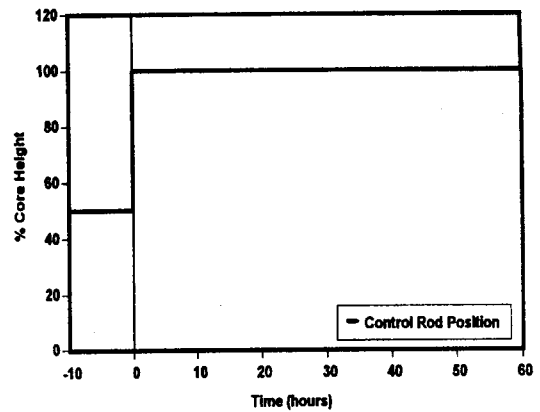


Fig. 2. Comparison of ASI Variation for Control Rod Withdrawal

4. Conclusions

A model of axial xenon oscillation due to control rod movement was suggested in this study. The model characterized the xenon oscillation in terms of axial difference parameters. An inhomogeneous equation system resulting from the control rod movement was derived from the two-group, one-dimensional neutron balance equations and iodine and xenon dynamics equations. The equation system can then be converted into a homogeneous equation system by defining rodged equilibrium axial power difference and the result gives a more general representation of xenon oscillation than

that of the previous work which does not include control rod considerations.[12] It was shown that the effect of control rod movement can be represented by rodged equilibrium axial power difference, initial axial power perturbation and its derivative. This makes it possible to initialize iodine and xenon with minimized pre-determined data and measured axial power difference data. The accuracy of the model was benchmarked via one-dimensional core calculation, and the results verified that the model provides good accuracy in predicting the trend of xenon oscillation behavior.

References

1. D. Randall and D. S. St. John, "Xenon Spatial Oscillations," *Nucleonics* 16, 82 (1958).
2. J. Chernick, "The Dynamics of a Xenon-Controlled Reactor," *Nucl. Sci. Eng.*, 8, 233 (1960).
3. S. G. Margolis and S. Kaplan, "Nonlinear Effects on Spatial Power Distribution Transients and Oscillations with Xenon Reactivity Feedback," WAPD-BT-21, 23, Bettis Atomic Power Laboratory (1960).
4. G. S. Lellouche, "Space Dependent Xenon Oscillations," *Nucl. Sci. Eng.*, 12, 482 (1962).
5. J. Canosa and H. Brooks, "Xenon-Induced Oscillations," *Nucl. Sci. Eng.*, 26, 237 (1966).
6. W. M. Stacey, "A Linear Analysis of Xenon Oscillation," KAPL-M-6596, Knolls Atomic Power Laboratory (1967).
7. R. A. Rydin, "Higher Flux Mode Effects in Xenon Spatial Oscillations," *Nucl. Sci. Eng.*, 50, 147 (1973).
8. R. J. Onega and R. A. Kisner, "An Axial Xenon Oscillation Model," *Annals of Nuclear Energy*, 5, 13 (1978).
9. R. J. Onega and R. A. Kisner, "Parameter Identification for Spatial Xenon Transient Analysis and Control," *Annals of Nuclear Energy*, 6, 369 (1979).
10. N. Z. Cho and L. M. Grossman, "Optimal Control for Xenon Spatial Oscillation in Load Follow of a Nuclear Reactor," *Nucl. Sci. Eng.*, 83, 136 (1983).
11. J. S. Song, N. Z. Cho, B. H. Lee, and S. Q. Zee, "Analytic Initialization of Non-Equilibrium Iodine and Xenon Distributions for Core Transient Simulation," *Nuclear Technology*, 116, 137 (1996).
12. J. S. Song and N. Z. Cho, "Two-Group, Flux-Coupled Xenon Oscillation Model with an Equation System of Axial Difference Parameters," *Nuclear Technology*, 119, 105 (1997).
13. "Users' s Manual ACE/ONED," KAERI/TR-631/96, Korea Atomic Energy Research Institute, (1996).